ACS APPLIED MATERIALS & INTERFACES

www.acsami.org Research Article

Electrochemically Enabled Embedded Three-Dimensional Printing of Freestanding Gallium Wire-like Structures

Xinpeng Wang, Xiao Liu, Peng Bi, Yingying Zhang, Liangtao Li, Jiarui Guo, Yang Zhang, Xufeng Niu, Yang Wang, Liang Hu,* and Yubo Fan*

Cite This: ACS Appl. Mater. Interfaces 2020, 12, 53966–53972 Read Online

ACCESS | Metrics & More | Article Recommendations | Supporting Information

ABSTRACT: The ability to pattern planar and freestanding 3D metallic architectures would enable numerous applications, including flexible electronics, displays, sensors, and antennas. Low melting point metals, such as gallium, have recently drawn considerable attention especially in the fields of flexible and stretchable electronics and devices owing to its unique properties, such as excellent electrical conductivity and fluidity. However, the large surface tension, low viscosity, and large density pose great challenges to 3D printing of freestanding gallium structures in a large scale, which hinder its further applications. In this article, we first propose an electrochemically enabled embedded 3D printing (3e-3DP) method for creating planar and freestanding gallium wire-like structures assisted with supporting hydrogel. After an enhanced solidification process and the removal of hydrogel, various freestanding 2D and 3D wire-like structures are realized. By simply reassembling the gallium structure into soft elastomer, a gallium-based flexible conductor and a 3D-spiral pressure sensor are demonstrated. Above all, this study presents a brand-new and economical way for the fabrication of 2D and 3D freestanding gallium structures, which has great prospects in wide applications in flexible and stretchable electronics and devices.

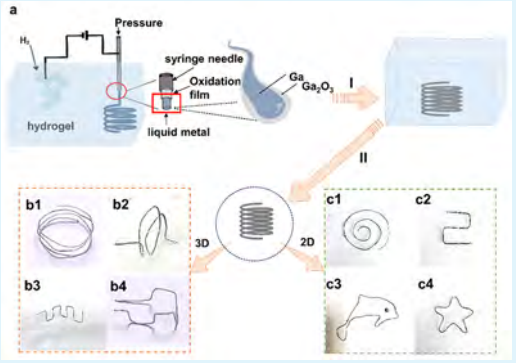

KEYWORDS: *liquid gallium, electrochemically enabled embedded 3D printing, freestanding gallium structure, flexible electronics, pressure sensor*

INTRODUCTION

The ability to pattern planar and freestanding three-dimensional (3D) metallic architectures would enable numerous applications, including flexible electronics,[1] biosensors,[2−4] aerospace industries,[5] construction,[6] etc. The past two decades have witness the significant advances in the field of 3D printing of metallic materials. To build metallic freestanding architectures from powder, wire, sheets, or ink, different techniques have been developed, including the electron beam melting, directed energy deposition,[7] and selective laser melting.[8,9] However, these approaches usually depend on large and complex instruments at a high cost and high energy consumption, which is not efficient and economical for mass production. In addition, currently only a small range of metal materials can be applicable to these techniques, which further constrain their applications.

Gallium, a metal with the melting point at around 29.8 °C, recently has attracted extensive attentions from researchers especially in the field of flexible electronics and wearable devices.[10,11] Apart from the desirable properties such as high electrical conductivity and good ductility that share with other flexible conductive materials, the transformable mechanical property of gallium can enable the reversible transition between the rigid static state and the flexible reconfigurable state of devices, which can accommodate versatile systems for more diverse applications.[12−16] As many electronic devices, such as inductors, capacitance, and antennas, work more efficiently in 3D forms, the 3D printing of freestanding gallium structures in an ambient environment present a great value especially in the applications such as wearable electronics and biomedical devices.

As gallium is solid at room temperature, it can be easily melted as liquid metal printing ink by heat transfer, which is inexpensive, convenient, and energy-saving compared with laser or electron melting techniques. Several studies have been reported to print 3D gallium-based liquid metal structures either in a supporting matrix or in an ambient environment.[17−19] However, due to the large surface tension of liquid metals, they often form droplets after extrusion from the nozzle, which significantly influence the printing resolution. The surface oxide over the liquid metals forming in the

Received: September 12, 2020
Accepted: October 29, 2020
Published: November 12, 2020

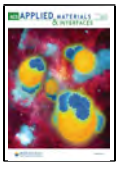

https://dx.doi.org/10.1021/acsami.0c16438
ACS Appl. Mater. Interfaces 2020, 12, 53966–53972

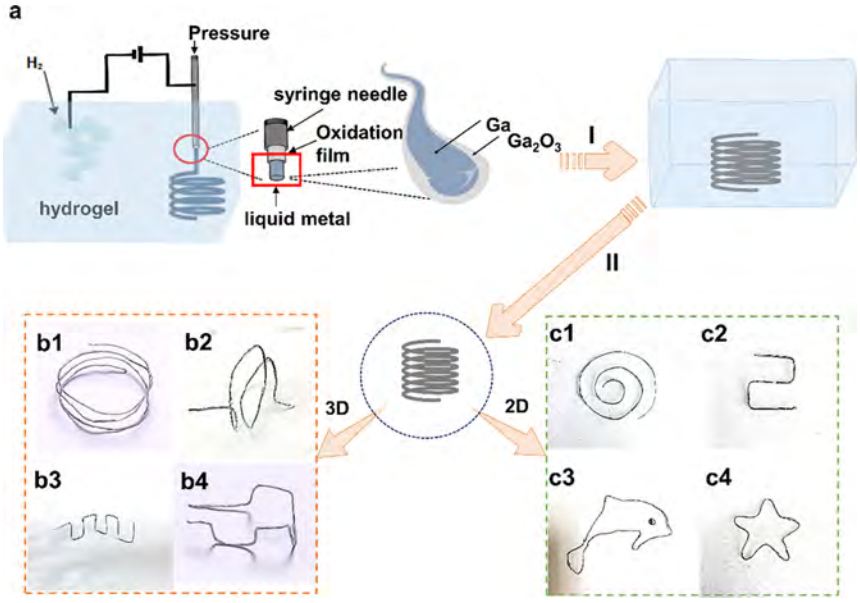

Figure 1. (a) Schematic procedure of the 3e-3DP for creating freestanding 3D gallium wire-like structures; I: the solidification process, II: the extraction process. (b1−b4) Freestanding gallium 3D structures and (c1−c4) freestanding gallium 2D patterns.

presence of air may help to support the fine shape and even freestanding structures in some degree. However, the load-bearing capacity of such thin oxide layer is far from being enough for even slightly larger structures, say about several centimeters high. In addition, due to the low melting point of EGaIn or GaInSn, it is difficult to transfer the printing structures from other substrates or matrix unless being completely solidified. Moreover, the solidification of gallium remains an issue. Due to the relatively large supercooling degree of gallium, it requires a much lower temperature and longer time for complete solidification, which also present difficulties in creating freestanding gallium structures.[20] In short, those intrinsic properties of gallium pose severe challenges for its wide applications in 3D printing.

In the present study, to fabricate planar and freestanding gallium wire-like structures with large size and high resolution, we propose an electrochemically enabled embedded 3D printing (3e-3DP) method. A convenient solidification process is also developed to effectively transfer the printing gallium structure from hydrogel. Briefly, this method involves extruding liquid gallium through a deposition nozzle into a supporting hydrogel (Figure 1). By electrochemically inducing a layer of surface oxide over the liquid gallium, we shape the liquid gallium into continuous wires with same diameters instead of small droplets. With the help of a supporting matrix, various 2D patterns and 3D structures such as spring coils are made. After an enhanced solidification process and the removal of the supporting matrix, the solidified gallium structures can be freestanding in an ambient environment. With the high conductivity and good ductility, these gallium structures can be reassembled into elastomers in a seamless manner to fabricate a flexible conductor and pressure sensors, which is more versatile, convenient, and highly adaptive to various applications.

RESULTS AND DISCUSSION

To enable this 3e-3DP, we developed a multicomponent 3D printing system, composed of a 3D printer, a DC power source, and a reservoir filled with conductive supporting hydrogel prepared with $CaCl_2$, gelatin, and water. The schematic diagram of this printing system is depicted in Figure 1a. The anode of electrical power is connected with the extrusion needle, and the cathode is put into the hydrogel. The printing ink, Ga, is extruded into the supporting self-healing hydrogel. Under a DC voltage, the electrochemical hydrolysis of the electrolyte is observed, during which the liquid metal (LM) acts as a liquid anode.[21] When connected with electricity, the reactions happened as follows.

$$Ga - 3e^- \rightarrow Ga^{3+} \quad (1)$$

$$3H_2O + 3e^- \rightarrow 3H_2 + 3OH^- \quad (2)$$

Also, anodic products such as Cl_2 are also produced at the LM surface in the hydrogel, $CaCl_2$ as the cross-linker. A DC voltage source is used to control electrochemical oxidation of liquid gallium, and then the surface tension of LM is declined.[21−24] It has been reported that the electrochemical extrusion of liquid metals can form wires in electrolyte solutions such as NaCl or NaOH, which is due to the electrochemically induced surface oxide formation (electro-capillary mechanism).[21,22] However, it is still challenging to form stable and fine LM wire-like patterns especially in 3D forms as the LM wires easily slip and sink within those solutions. Hence, those LM wires require quick solidification to maintain its wire-like structure, otherwise they easily transform into droplets even when the oxide layer is formed.[21−26] In our study, we successfully fabricate gallium wire-like structures in 3D forms by this 3e-3DP method (Movie S1), in which the conductive self-healing hydrogel not only provides the electrolyte surroundings but also mechanically supports the heavy gallium structures. Thus, the liquid gallium 3D structures can be suspended in the hydrogel during the printing process. Then, the gallium structure is solidified at room temperature by an enhanced solidification method (step I in Figure 1a) and is taken out from melted hydrogel by heating at 28 °C (step II). The solidified freestanding gallium is exhibited in Figure 1b,c, including the 3D spring-like structures with the same diameter (Figure 1b1), different

https://dx.doi.org/10.1021/acsami.0c16438
ACS Appl. Mater. Interfaces 2020, 12, 53966−53972

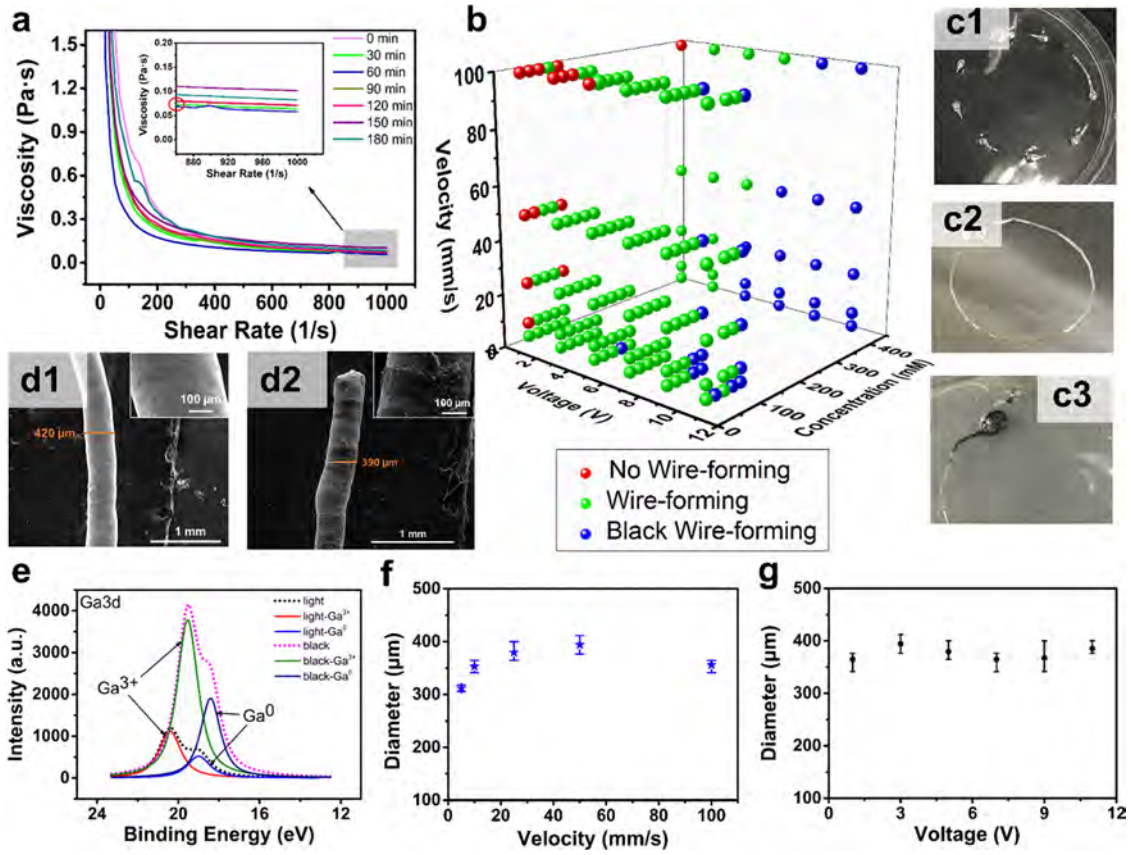

Figure 2. (a) Viscosity of gelatin hydrogel in our printing system. (b) Wire-forming conditions ($CaCl_2$ concentration, voltage, and velocity). (c1−c3) Photographs of no wire-forming, wire-forming, and black wire-forming, respectively. (d1, d2) SEM images of the printed liquid metal oxide layer and blackened oxide layer at 100 and 1000 magnifications, respectively. (e) Ga3d XPS of printed gallium without or with the black oxide layer. (f, g) Relationship between wire diameter and velocity, and voltage, respectively.

diameters (Figure 1b2), 2D helix (Figure 1c1), arch (Figure 1c2), and relative structures and patterns. These freestanding gallium structures demonstrate the feasibility of this printing method in creating complicated gallium 3D structures in a simple way.

To obtain continuous liquid gallium wire-like structures with high-fidelity in the supporting hydrogel, several criteria must be well fulfilled. First, the liquid gallium wire formation depends on the electrochemical surface oxidation, which must be precisely controlled. Second, the rheological properties of the hydrogel must be well tuned to be able to support the heavy gallium as well as to be self-healable.[27,28] Based on the preliminary studies, the concentration of gelatin, 5% w/w, was chosen in the follow-up experiments. At a lower concentration (2%), it requires a long time to cross-link and reach the right condition for printing, while at 10%, it is quickly fully cross-linked before printing and is not self-healable. The viscosity of the printing hydrogel possesses a shear thinning behavior, and the rheological properties is generally stable within 2 h at room temperature (around 26 °C) (Figure 2a). The liquid gallium wire can suspend in the hydrogel without obvious sinking within almost 2 h. Thus it can provide a general stable supporting surrounding during printing.

To further clarify the wire-forming condition, multifactors are overall evaluated, including the voltages applied, the $CaCl_2$ concentration, and the motion velocity of the nozzle. In this study, the extruded velocity is fixed at 200 μL/min based on our experiments, and the inner diameter of the needle-like nozzle is 0.61 mm. It is generally considered that the extrusion speed of the liquid gallium approximately equals to the movement of the nozzle. Otherwise, the wires can easily break due to the speed mismatch. By large numbers of trials, the liquid gallium wire-forming conditions are summarized as shown in Figure 2b. Generally, it is more likely to form wire at a low speed of the nozzle since the liquid gallium wire is more likely to break when being dragged by the nozzle. In this study, the gallium wires can form at a low voltage (1 V) and low $CaCl_2$ concentration. When the voltage or the $CaCl_2$ concentration is too low, liquid gallium droplets form instead of wires (Figure 2c1). In the voltage range of 1−7 V, with appropriate velocity, the wires can be formed without a black layer (Figure 2)c2 . When the voltage is too large (over 9 V), liquid gallium wires form with obvious dark layers (Figure 2c3), which is unstable on the surface after shaking, a higher voltage, or adding acid/alkali solution. This is in accordance to the phenomenon in a previous work, which may be due to the dealloying of gallium when flowing through the stainless steel syringe needle during the application of the voltage.[26,29] The SEM images of the dark layer presents wrinkled appearance over the wire (Figure 2d1,d2), which is demonstrated to contain much higher gallium oxide than that at small voltages by XPS characterization (Figure 2e and Figure S1). From XPS of Ga3d (Figure 2e), it is obvious that the layer is formed by the metal oxide (20.7 eV). Also, in XPS of the O element (Figure S1), it also reveals the existence of gallium oxide (530.8 eV) for the black layer. Meanwhile, without the black

https://dx.doi.org/10.1021/acsami.0c16438
ACS Appl. Mater. Interfaces 2020, 12, 53966−53972

layer, due to the adsorbed water on the hydrophilic gallium oxide layer, the peak is at 531.6 eV ($OH-H_2O$), which is maybe called hydrated gallium oxide. This result is consistent with previous studies.[24,30] The SEM of solidified liquid metal is observed in Figure S2, which shows the black oxide layer is nonuniform. No other change can be seen with the black oxide layer in the whole XPS characterization (Figure S3).

Although the inner diameter of the nozzle is fixed, the diameter of wires (minimum diameter is around 300 μm) is observed to be slightly affected by the nozzle velocity (Figure 2f). Under a fixed $CaCl_2$ concentration and printing depth, the diameter of wire slightly increase with the nozzle velocity (5−50 mm/s). The reason maybe is that with the constant extrusion floxion of liquid gallium, the liquid metal has a trend to fall and accumulate at lower velocity to make the wire diameter smaller. While, at high velocity (>50 mm/s), the liquid metal is quickly stretched and flows out with high surface tension to form wire so that the diameter gets smaller. Other factors, such as applied voltages and printing depth, are also studied and found to have negligible effects on the wire diameter (Figure 2g and Figure S4). Through the above exploration, we selected optimized experimental conditions (3 V, 40 mM, 50 mm/s, >1 mm depth) for subsequent experiments.

To acquire freestanding gallium wire-like structures, the liquid gallium should be solidified and be removed from the hydrogel. However, due to the supercooling effect, the extremely low temperature (<−20 °C) and a long time are required for the solidification of liquid gallium in the hydrogel (Figure S5). In the present study, we overcome the supercooling effect by making the solid gallium wire contact with the liquid gallium, which works as a nucleating agent and facilitates the nucleation during solidificaiton.[31] As illustrated in Figure 3a, the metal freezes, starting at the nucleation site

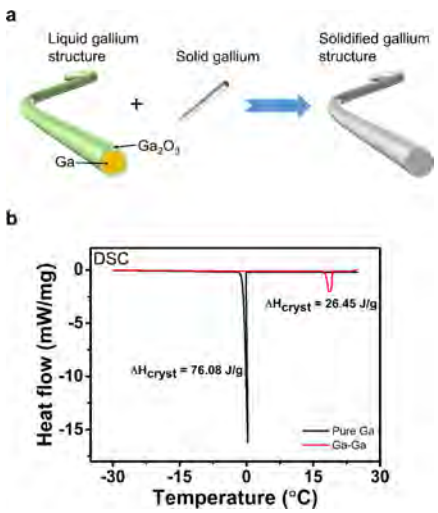

Figure 3. (a) Solidification process of liquid gallium. (b) DSC of pure Ga and adding Ga as a nucleating agent.

and propagating along the fiber.[32] The solidified velocity is around 3 mm/s when the wire diameter is 400 μm. After solidified in hydrogel, the whole gallium structure can be easily removed from the hydrogel by heating at 28 °C, when the hydrogel melts while the gallium is solid. The differential scanning calorimetry (DSC) is implemented through 5 °C/min. The results suggest the freezing point of gallium with metal particles (around 20 °C) is dozens of degrees higher than the pure gallium (Figure 3b). Also, the enthalpy change (ΔH_{cryst}) is much lower than that of pure gallium, which means that it is easier to be solidified. Apart from solid gallium, the surface oxide or the hydrogel may also enhance the solidification process. Thus, the pure liquid gallium wires can be easily solidified at around 0 °C in the present study.

Owning to the specific melting point, solid gallium structures can easily melt at body temperature, which have inspired a series of mechanically transformative electronics, sensors, and implantable devices.[3,11,33−35] In the present study, freestanding 2D and 3D gallium structures can be printed, which offers more possibilities for the fabrication of electronics or devices for broaden applications. As one of the conceptual demonstrations, the flexible conductor is conveniently fabricated in two steps (Figure 4a). The connectivity is tested

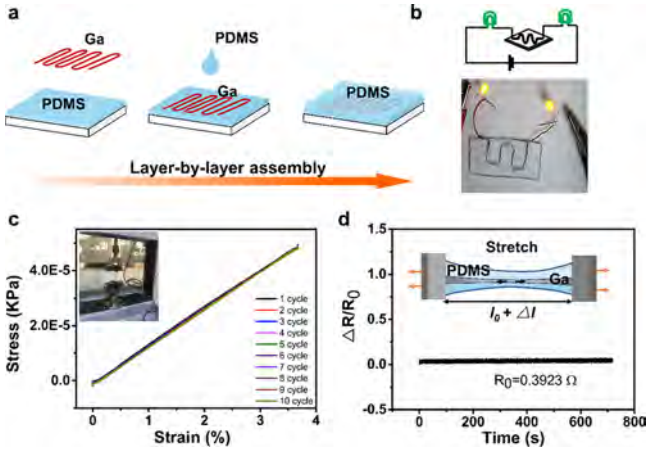

Figure 4. (a) Encapsulation process of liquid gallium. (b) Schematic diagram and photo of the LED qualitative connectivity test. (c) Strain−stress curve under 10 cycles of repeated stretching. (d) Resistance change under a stretched condition, with a deformation diagram inserted.

and verified by using an LED bulb (Figure 4b). Apparently, the surface oxide layer forms on gallium, which has been proved that it forms as long as the concentration of oxygen is greater than ppm levels and forms almost instantly in air at ambient conditions.[25] Moreover, as reported before, liquid metals have good self-healing performance due to its excellent extensibility and high surface tension, which enable instantaneous and repeatable self-healing of their electrodes (within a few milliseconds) under no external energy as well as high stretchability.[36] So that after being cut off and reconnected, the flexible conductor still can continue to work (Movie S2), which is advantageous for their applications in deformable electronics. Under stretching and pressure, the principle about the resistance of liquid metal $R = \rho l/s$, and the volume of liquid metal $V = l \times s$, so $R = \rho l/s = \rho l^2/V$.[37] The stress−strain curve after stretching is detected in Figure 4c (with the actual photo inserted), which shows the feasibility in the application on mechanically transformative devices. Also, when stretched along its axial direction (Figure 4d), the channel structure inside PDMS substrate deformed into a concave shape; hence, the both ends of liquid metal became convex, the width d of liquid metal pattern decreased, while the length l of the liquid metal pattern increased. With a very small initial resistance (R_0 = 0.3923 Ω), the resistance shows little change under

https://dx.doi.org/10.1021/acsami.0c16438
ACS Appl. Mater. Interfaces 2020, 12, 53966−53972

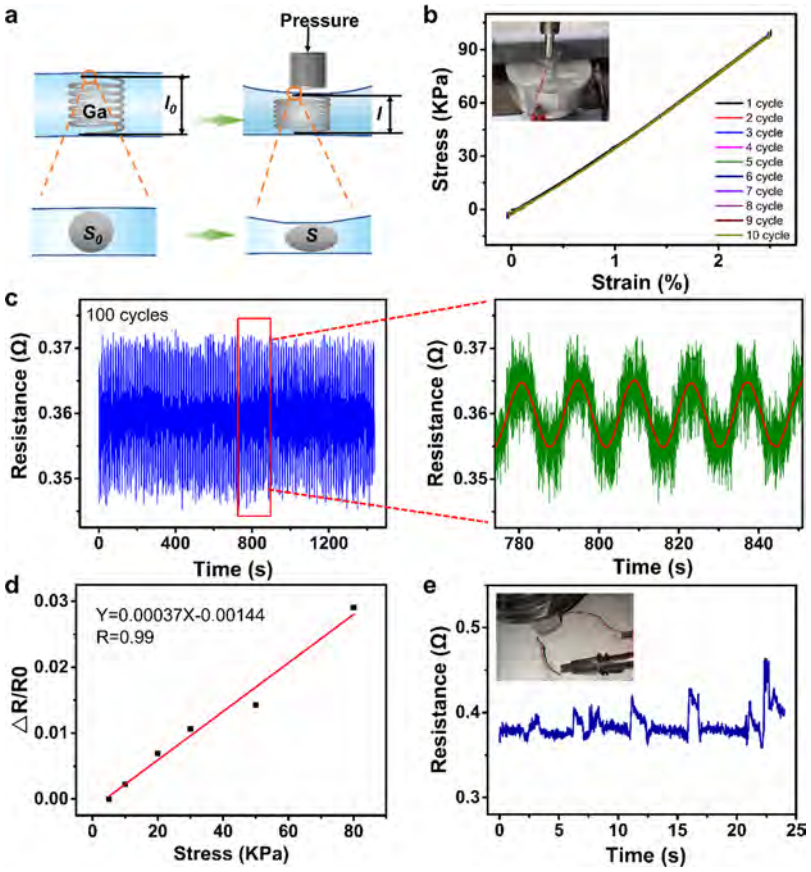

Figure 5. (a) Pressure sensor based on freestanding gallium spiral. (b) Strain−stress curve under pressure. (c) Resistance change after 100 cycles of repeated compressing. (d) Resistance change under different pressures. (e) Resistance change while pressed by the shoes.

stretching (5 N, Figure 4d), which can be used in flexible electronics.

Specially, taking advantage of this 3e-3DP method, a pressure sensor based on a printed gallium spiral is presented as another conceptual demonstration. This sensor is prepared in the same way as above. Also, the principle is shown in Figure 5a; under pressure along its vertical direction, the liquid gallium structure deformed, leading to a significant reduction in the cross-sectional area of the microchannel. Based on the fomula $R = \rho l/s$, the resistivity ρ and volume V was unchanged, so the decrease of l and s resulted in the increase of R. The sprial is 1.2 cm in diameter and 1.5 cm in height, and the encapsulated sensor is 1.5 cm in length and 1.8 cm in height. By pressing this sensor in the vertical way, the spiral is compressed and the resistance varied with this deformation. The stress−strain curve under pressure is detected and shows excellent resilience without residual stress as shown in Figure 5b. The resistance along with the pressure is measured, which present good repeatability and linearity (Figure 5c,d). As shown in Figure 5c, during compressing cycles, resistance change remains consistent at a maximum upon 100 cycles of repeated compressing. The sensitivity (S) can be obtained by the equation of $S = \delta(\Delta R/R_0)/\delta P$,[38] ΔR is the value of resistance change, R_0 is the value of initial resistance, and P is the value of pressure. The sensor exhibited excellent sensing performance with high sensitivity and stability (3.7×10^{-4} kPa^{-1} under a pressure of 5−80 kPa, see Figure 5d and Figure S6). Similarly, it can be used to monitor the pressure changes in real time, such as the foot pressure detection (Figure 5e).

CONCLUSIONS

To sum up, we report a new method termed as electrochemically enabled embedded 3D printing (3e-3DP) for creating freestanding 2D and 3D gallium wire-like structures at large scales. The printing conditions are explored and optimized, including the applied voltage, the supporting hydrogel, and the nozzle speed. As a result, various gallium freestanding 2D patterns and 3D structures are achieved, which is also a benefit for the subsequent device fabrication process. This printing technique is fast and inexpensive, which is applicable in laboratories, homes, and industries. Combined with the intriguing properties of liquid gallium, such as unique melting point, high mobility, and electrical conductance, a flexible conductor and a pressure sensor are demonstrated. This 3e-3DP method opens a brand-new way for gallium shaping in 2D and 3D forms, which can inspire more applications in flexible, stretchable, and self-healable electronics and devices.

EXPERIMENTAL SECTION

Materials and Methods. The experiments were carried out on the liquid metal (gallium, Ga). Ga with a purity of 99.99% was added into a beaker and heated to 100 °C. Ga was used in the subsequent experiments. Gelatin and calcium chloride ($CaCl_2$) were purchased from BOSF. Deionized water (Milli-Q System, Millipore, U.S.A.) was used in all experiments. Polydimethylsiloxane (PDMS, Sylgard 184) was purchased from Dow Corning Corp. (U.S.A.).

Printing and Encapsulated Methods. The printing system was fabricated by three parts, including a 3D printing system, voltage stabilizer, and an injection pump. For each experiment, the printing needle was moving in the supporting hydrogel medium along

https://dx.doi.org/10.1021/acsami.0c16438
ACS Appl. Mater. Interfaces 2020, 12, 53966−53972

programmed paths, which was controlled by G-code commands generated through model conversion software (Slic3r) from STL files designed using a CAD system (SolidWorks) and standard 3D printing software (Repetier-Host). Also, the 2D pattern was controlled by the printer through the PLT file. PDMS was used as an encapsulated material. A spin coater (TB-616) was used to form the wearable devices. To facilitate subsequent resistance detection, during the solidification process of PDMS, Cu thin wires could be inserted to connect with Ga. Finally, the insert hole was encapsulated by PDMS.

Photography and Characterization Methods. Photographs were taken using a digital camera (EOS 70D, canon) under a bright field. The sizes of liquid metal wires were imaged and measured using an inverted optical microscope (Axio Observer Z1, Carl Zeiss). The rheological behavior of gelatin hydrogel was detected by the a viscosity meter (RHEO3000). The prepared solidified liquid metal wires were cleaned using deionized water and dried at room temperature for 24 h, and then its morphology and elemental analysis were examined using a field emission scanning electron microscope (SEM, ZEISS Ultra 55). An ESCALAB 250 X-ray photoelectron spectrometer (XPS, Thermo Fisher Scientific Company, U.S.A.) was used to test the chemical compositions of LM prepared by electronic printing. A differential scanning calorimeter (DSC, Mettler DSC III) was used to measure the freezing and melting temperature points of pure gallium and gallium with the nucleating agent. To further investigate the electrical properties of the liquid metal embedded in the PDMS substrate, continuous pressure and tension were applied using a universal testing machine (AGS-X, Shimadzu, Japan) for full loading−unloading cycles. To apply the pressure on the pressure-sensing area of the sensor, an acryl cube with a contact area of 10 × 10 mm was placed on the sensor. The pressure and tension were applied with a loading speed of 0.1 mm s^{-1}, while the corresponding resistance was measured using a source meter (Keithley 2400, Tektronix, U.S.A.).

■ ASSOCIATED CONTENT

Supporting Information

The Supporting Information is available free of charge at https://pubs.acs.org/doi/10.1021/acsami.0c16438.

(Figure S1) O 1s X-ray photoelectron spectroscopy (XPS) of printed liquid gallium with (red) or without (blue) a black layer; (Figure S2) SEM of printed and solidified liquid metal with an oxide layer (a) and blackened oxide layer (b) at 100 and 1000 magnifications, respectively; (Figure S3) X-ray photoelectron spectroscopy (XPS) of printed liquid gallium with (a) or without (b) a black layer; (Figure S4) the relationship between wire diameter and printing depth; (Figure S5) the unsolidified graph of liquid gallium in the hydrogel at −20 °C for 6 h; (Figure S6) the resistance change of the prepared sensor under different pressures (PDF)

(Movie S1) The printing process of liquid gallium in hydrogel (MP4)

(Movie S2) The connectivity test of the sensor by using an LED bulb after cutting off and reconnecting MP4)

■ AUTHOR INFORMATION

Corresponding Authors

Liang Hu − *School of Biological Science and Medical Engineering, Key Laboratory for Biomechanics and Mechanobiology, Beihang Univeristy, Beijing 100083, China*; Email: cnhuliang@buaa.edu.cn

Yubo Fan − *School of Biological Science and Medical Engineering, Key Laboratory for Biomechanics and Mechanobiology, Beihang Univeristy, Beijing 100083, China*; Email: yubofan@buaa.edu.cn

Authors

Xinpeng Wang − *School of Biological Science and Medical Engineering, Key Laboratory for Biomechanics and Mechanobiology, Beihang Univeristy, Beijing 100083, China*; orcid.org/0000-0002-1583-314X

Xiao Liu − *School of Biological Science and Medical Engineering, Key Laboratory for Biomechanics and Mechanobiology, Beihang Univeristy, Beijing 100083, China*; orcid.org/0000-0003-3213-8357

Peng Bi − *Key Laboratory of Organic Optoelectronics and Molecular Engineering of the Ministry of Education, Department of Chemistry and Center for Nano and Micro Mechanics (CNMM), Tsinghua University, Beijing 100084, P.R. China*

Yingying Zhang − *Key Laboratory of Organic Optoelectronics and Molecular Engineering of the Ministry of Education, Department of Chemistry and Center for Nano and Micro Mechanics (CNMM), Tsinghua University, Beijing 100084, P.R. China*; orcid.org/0000-0002-8448-3059

Liangtao Li − *School of Biological Science and Medical Engineering, Key Laboratory for Biomechanics and Mechanobiology, Beihang Univeristy, Beijing 100083, China*

Jiarui Guo − *School of Biological Science and Medical Engineering, Key Laboratory for Biomechanics and Mechanobiology, Beihang Univeristy, Beijing 100083, China*; orcid.org/0000-0002-8965-1365

Yang Zhang − *School of Biological Science and Medical Engineering, Key Laboratory for Biomechanics and Mechanobiology, Beihang Univeristy, Beijing 100083, China*

Xufeng Niu − *School of Biological Science and Medical Engineering, Key Laboratory for Biomechanics and Mechanobiology, Beihang Univeristy, Beijing 100083, China*

Yang Wang − *School of Biological Science and Medical Engineering, Key Laboratory for Biomechanics and Mechanobiology, Beihang Univeristy, Beijing 100083, China*

Complete contact information is available at: https://pubs.acs.org/10.1021/acsami.0c16438

Notes

The authors declare no competing financial interest.

■ ACKNOWLEDGMENTS

This work is supported by the 111 Project (project no. B13003), the National Natural Science Foundation of China (grant nos.81801794, 11827803, and 11421202), and the Natural Science Foundation of Beijing (grant no.7202014).

■ REFERENCES

(1) Martin, J. H.; Yahata, B. D.; Hundley, J. M.; Mayer, J. A.; Schaedler, T. A.; Pollock, T. M. 3D Printing of High-Strength Aluminium Alloys. *Nature* **2017**, *549*, 365−369.

(2) Hensleigh, R.; Cui, H.; Xu, Z.; Massman, J.; Yao, D.; Berrigan, J.; Zheng, X. Charge-Programmed Three-Dimensional Printing for Multi-Material Electronic Devices. *Nat. Electron.* **2020**, *3*, 216−224.

(3) Yu, Y.; Zhang, J.; Liu, J. Biomedical Implementation of Liquid Metal Ink as Drawable ECG Electrode and Skin Circuit. *PLoS One* **2013**, *8*, No. e58771.

(4) Zhang, D.; Qiu, D.; Gibson, M. A.; Zheng, Y.; Fraser, H. L.; StJohn, D. H.; Easton, M. A. Additive Manufacturing of Ultrafine-Grained High-Strength Titanium Alloys. *Nature* **2019**, *576*, 91−95.

(5) Koons, G. L.; Diba, M.; Mikos, A. G. Materials Design for Bone-Tissue Engineering. *Nat. Rev. Mater.* **2020**, *5*, 584−603.
(6) Buchanan, C.; Gardner, L. Metal 3D Printing in Construction: A Review of Methods, Research, Applications, Opportunities and Challenges. *Eng. Struct.* **2019**, *180*, 332−348.
(7) Maurel, A.; Grugeon, S.; Fleutot, B.; Courty, M.; Prashantha, K.; Tortajada, H.; Armand, M.; Panier, S.; Dupont, L. Three-Dimensional Printing of a $LiFePO_4$/Graphite Battery Cell via Fused Deposition Modeling. *Sci. Rep.* **2019**, *9*, 18031.
(8) Skylar-Scott, M. A.; Gunasekaran, S.; Lewis, J. A. Laser-assisted Direct Ink Writing of Planar and 3D Metal Architectures. *Proc. Natl. Acad. Sci. U. S. A.* **2016**, *113*, 6137−6142.
(9) Zglobicka, I.; Chmielewska, A.; Topal, E.; Kutukova, K.; Gluch, J.; Krüger, P.; Kilroy, C.; Swieszkowski, W.; Kurzydlowski, K. J.; Zschech, E. 3D Diatom−Designed and Selective Laser Melting (SLM) Manufactured Metallic Structures. *Sci. Rep.* **2019**, *9*, 19777.
(10) Daalkhaijav, U.; Yirmibesoglu, O. D.; Walker, S.; Mengüç, Y. Rheological Modification of Liquid Metal for Additive Manufacturing of Stretchable Electronics. *Adv. Mater. Technol.* **2018**, *3*, 1700351.
(11) Teng, L.; Zhu, L.; Handschuh-Wang, S.; Zhou, X. Robust, Multiscale Liquid-Metal Patterning Enabled by a Sacrificial Sealing Layer for Flexible and Wearable Wireless Powering. *J. Mater. Chem. C* **2019**, *7*, 15243−15251.
(12) Zhang, M.; Yao, S.; Rao, W.; Liu, J. Transformable Soft Liquid Metal Micro/Nanomaterials. *Mater. Sci. Eng., R* **2019**, *138*, 1−35.
(13) Wang, L.; Liu, J. Advances in the Development of Liquid Metal-Based Printed Electronic Inks. *Front. Mater.* **2019**, *6*, 303.
(14) Xu, Q.; Oudalov, N.; Guo, Q.; Jaeger, H. M.; Brown, E. Effect of Oxidation on the Mechanical Properties of Liquid Gallium and Eutectic Gallium-Indium. *Phys. Fluids* **2012**, *24*, No. 063101.
(15) Byun, S.-H.; Sim, J. Y.; Zhou, Z.; Lee, J.; Qazi, R.; Walicki, M. C.; Parker, K. E.; Haney, M. P.; Choi, S. H.; Shon, A.; Gereau, G. B.; Bilbily, J.; Li, S.; Liu, Y.; Yeo, W.-H.; McCall, J. G.; Xiao, J.; Jeong, J.-W. Mechanically Transformative Electronics, Sensors, and Implantable Devices. *Sci. Adv.* **2019**, *5*, eaay0418.
(16) Merhebi, S.; Mayyas, M.; Abbasi, R.; Christoe, M. J.; Han, J.; Tang, J.; Rahim, M. A.; Yang, J.; Tan, T. T.; Chu, D.; Zhang, J.; Li, S.; Wang, C. H.; Kalantar-Zadeh, K.; Allioux, F.-M. Magnetic and Conductive Liquid Metal Gels. *ACS Appl. Mater. Interfaces* **2020**, *12*, 20119−20128.
(17) Yu, Y.; Liu, F.; Zhang, R.; Liu, J. Suspension 3D Printing of Liquid Metal into Self-Healing Hydrogel. *Adv. Mater. Technol.* **2017**, *2*, 1700173.
(18) Park, Y.-G.; An, H. S.; Kim, J.-Y.; Park, J.-U. High-Resolution, Reconfigurable Printing of Liquid Metals with Three-Dimensional Structures. *Sci. Adv.* **2019**, *5*, eaaw2844.
(19) Park, Y.-G.; Min, H.; Kim, H.; Zhexembekova, A.; Lee, C. Y.; Park, J.-U. Three-Dimensional, High-Resolution Printing of Carbon Nanotube/Liquid Metal Composites with Mechanical and Electrical Reinforcement. *Nano Lett.* **2019**, *19*, 4866−4872.
(20) Wang, L.; Liu, J. Liquid Metal Material Genome: Initiation of a New Research Track towards Discovery of Advanced Energy Materials. *Front. Energy* **2013**, *7*, 317−332.
(21) Han, J.; Tang, J.; Idrus-Saidi, S. A.; Christoe, M. J.; O'Mullane, A. P.; Kalantar-Zadeh, K. Exploring Electrochemical Extrusion of Wires from Liquid Metals. *ACS Appl. Mater. Interfaces* **2020**, *12*, 31010−31020.
(22) Khan, M. R.; Eaker, C. B.; Bowden, E. F.; Dickey, M. D. Giant and Switchable Surface Activity of Liquid Metal via Surface Oxidation. *Proc. Natl. Acad. Sci. U. S. A.* **2014**, *111*, 14047−14051.
(23) Zhang, J.; Sheng, L.; Liu, J. Synthetically Chemical-Electrical Mechanism for Controlling Large Scale Reversible Deformation of Liquid Metal Objects. *Sci. Rep.* **2014**, *4*, 7116.
(24) Wang, H.; Yuan, B.; Liang, S.; Guo, R.; Rao, W.; Wang, X.; Chang, H.; Ding, Y.; Liu, J.; Wang, L. PLUS-M: a Porous Liquid-Metal Enabled Ubiquitous Soft Material. *Mater. Horiz.* **2018**, *5*, 222−229.
(25) Dickey, M. D. Emerging Applications of Liquid Metals Featuring Surface Oxides. *ACS Appl. Mater. Interfaces* **2014**, *6*, 18369−18379.
(26) Mayyas, M.; Mousavi, M.; Ghasemian, M. B.; Abbasi, R.; Li, H.; Christoe, M. J.; Han, J.; Wang, Y.; Zhang, C.; Rahim, M. A.; Tang, J.; Yang, J.; Esrafilzadeh, D.; Jalili, R.; Allioux, F.-M.; O'Mullane, A. P.; Kalantar-Zadeh, K. Pulsing Liquid Alloys for Nanomaterials Synthesis. *ACS Nano* **2020**, 14070.
(27) Xu, J.; Wang, Z.; You, J.; Li, X.; Li, M.; Wu, X.; Li, C. Polymerization of Moldable Self-Healing Hydrogel with Liquid Metal Nanodroplets for Flexible Strain-Sensing Devices. *Chem. Eng. J.* **2020**, *392*, 123788.
(28) He, Q.; Huang, Y.; Wang, S. Hofmeister Effect-Assisted One Step Fabrication of Ductile and Strong Gelatin Hydrogels. *Adv. Funct. Mater.* **2018**, *28*, 1705069.
(29) Tang, J.; Zhao, X.; Li, J.; Zhou, Y.; Liu, J. Liquid Metal Phagocytosis: Intermetallic Wetting Induced Particle Internalization. *Adv. Sci.* **2017**, *4*, 1700024.
(30) Guo, J.; Cheng, J.; Tan, H.; Zhu, S.; Qiao, Z.; Yang, J.; Liu, W. Ga-Based Liquid Metal: A Novel Current-Carrying Lubricant. *Tribol. Int.* **2019**, *135*, 457−462.
(31) Bai, G.; Gao, D.; Liu, Z.; Zhou, X.; Wang, J. Probing the Critical Nucleus Size for Ice Formation with Graphene Oxide Nanosheets. *Nature* **2019**, *576*, 437−441.
(32) Park, S.; Baugh, N.; Shah, H. K.; Parekh, D. P.; Joshipura, I. D.; Dickey, M. D. Ultrastretchable Elastic Shape Memory Fibers with Electrical Conductivity. *Adv. Sci.* **2019**, *6*, 1901579.
(33) Liu, Y.; Yang, T.; Zhang, Y.; Qu, G.; Wei, S.; Liu, Z.; Kong, T. Ultrastretchable and Wireless Bioelectronics Based on All-Hydrogel Microfluidics. *Adv. Mater.* **2019**, *31*, 1902783.
(34) Muth, J. T.; Vogt, D. M.; Truby, R. L.; Mengüç, Y.; Kolesky, D. B.; Wood, R. J.; Lewis, J. A. Embedded 3D Printing of Strain Sensors within Highly Stretchable Elastomers. *Adv. Mater.* **2014**, *26*, 6307−6312.
(35) Kim, K.; Choi, J.; Jeong, Y.; Cho, I.; Kim, M.; Kim, S.; Oh, Y.; Park, I. Highly Sensitive and Wearable Liquid Metal-Based Pressure Sensor for Health Monitoring Applications: Integration of a 3D-Printed Microbump Array with the Microchannel. *Adv. Healthcare Mater.* **2019**, *8*, 1900978.
(36) Park, Y.-G.; Kim, H.; Park, S.-Y.; Kim, J.-Y.; Park, J.-U. Instantaneous and Repeatable Self-Healing of Fully Metallic Electrodes at Ambient Conditions. *ACS Appl. Mater. Interfaces* **2019**, *11*, 41497−41505.
(37) Hu, T.; Xuan, S.; Ding, L.; Gong, X. Liquid Metal Circuit Based Magnetoresistive Strain Sensor with Discriminating Magnetic and Mechanical Sensitivity. *Sens. Actuators, B* **2020**, *314*, 128095.
(38) Liao, M.; Liao, H.; Ye, J.; Wan, P.; Zhang, L. Polyvinyl Alcohol Stabilized Liquid Metal Hydrogel for Wearable Transient Epidermal Sensors. *ACS Appl. Mater. Interfaces* **2019**, *11*, 47358−47364.

NOTE ADDED AFTER ASAP PUBLICATION

This paper was published on the Web on November 12, 2020. Affiliation INSCA was removed from all authors in the paper and Supporting Information file, and the corrected version was reposted on November 18, 2020.

https://dx.doi.org/10.1021/acsami.0c16438
ACS Appl. Mater. Interfaces 2020, 12, 53966−53972